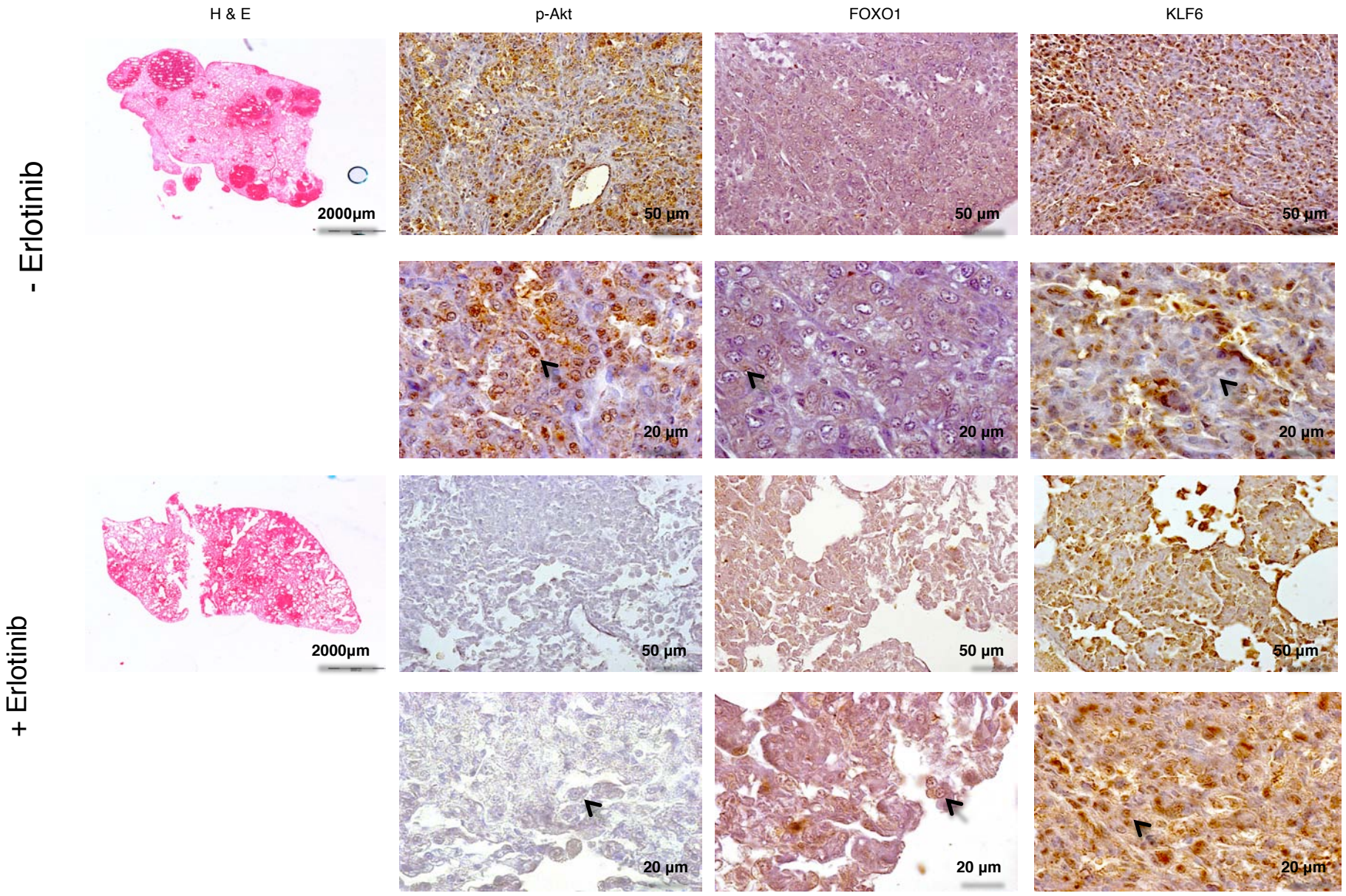

Supplemental Figure 1

Inhibition of activated EGFR signaling regulates FOXO1/KLF6 in the EGFR-L858R transgenic mouse model of lung adenocarcinoma. Paraffin embedded tissue sections, L858R mouse tumor samples after treatment with erlotinib compared to vehicle-treated control mice, were stained with H&E, pAKT, FOXO1, and KLF6. Mice treated with erlotinib expressed decreased p-AKT and led to FOXO1 and KLF6 nuclear relocalization. Arrows highlight a representative nuclei. Scale bar, 20 µm (100x-oil objective) and 50µm (40x-oil objective).

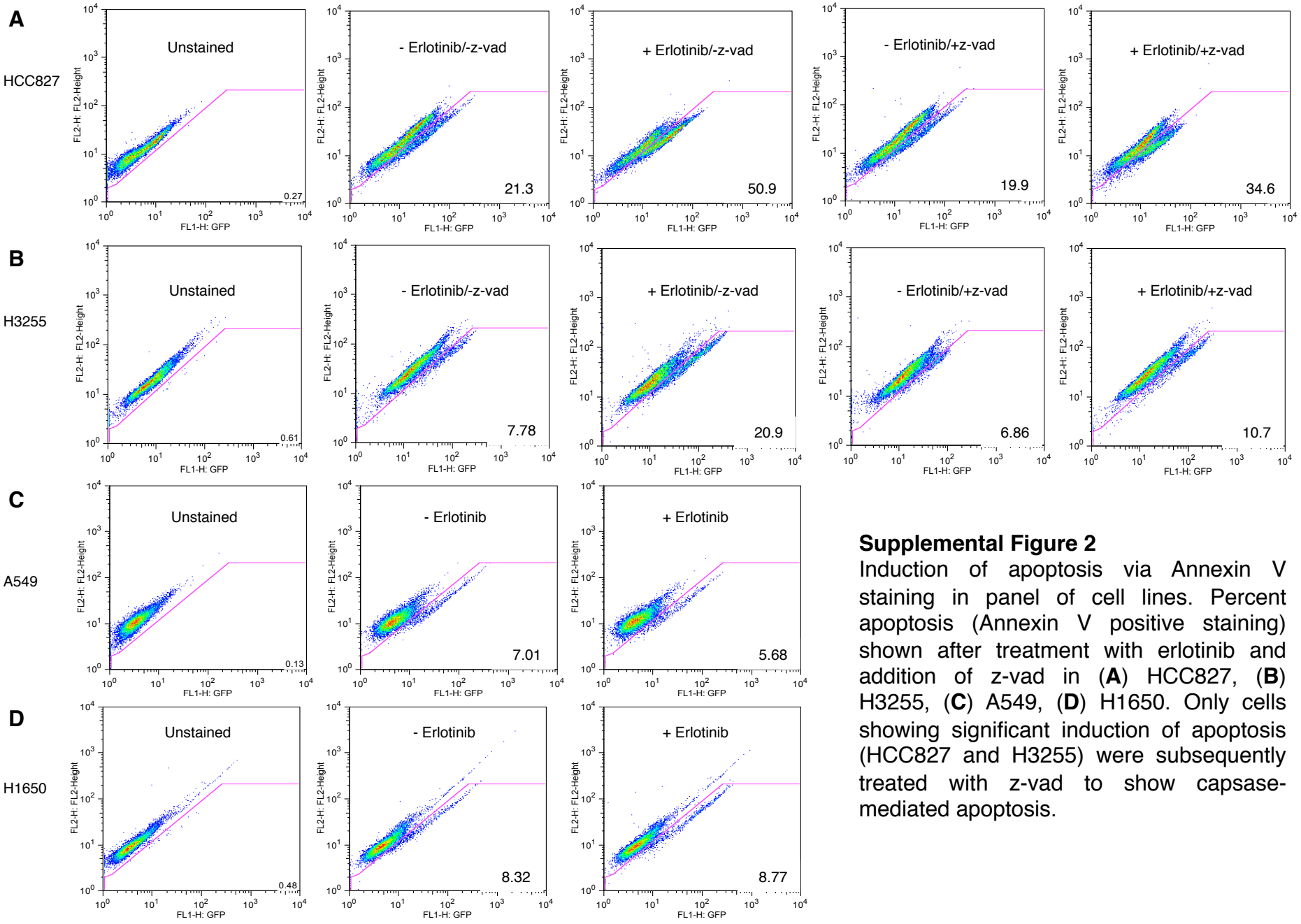

Supplemental Figure 2
Induction of apoptosis via Annexin V staining in panel of cell lines. Percent apoptosis (Annexin V positive staining) shown after treatment with erlotinib and addition of z-vad in (**A**) HCC827, (**B**) H3255, (**C**) A549, (**D**) H1650. Only cells showing significant induction of apoptosis (HCC827 and H3255) were subsequently treated with z-vad to show capsase-mediated apoptosis.

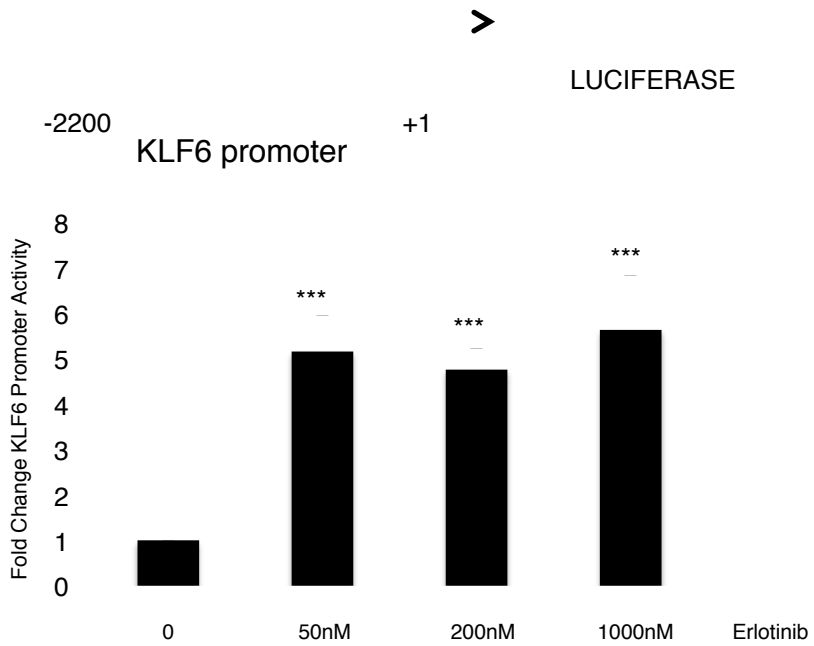

Supplemental Figure 3
Increase in KLF6 promoter activity upon treatment with erlotinib. KLF6 promoter activity assessed by a 2.2kb dual-luciferase reporter assay system in the erlotinib sensitive HCC827 cell line 24 hours after the addition of increasing doses of erlotinib.

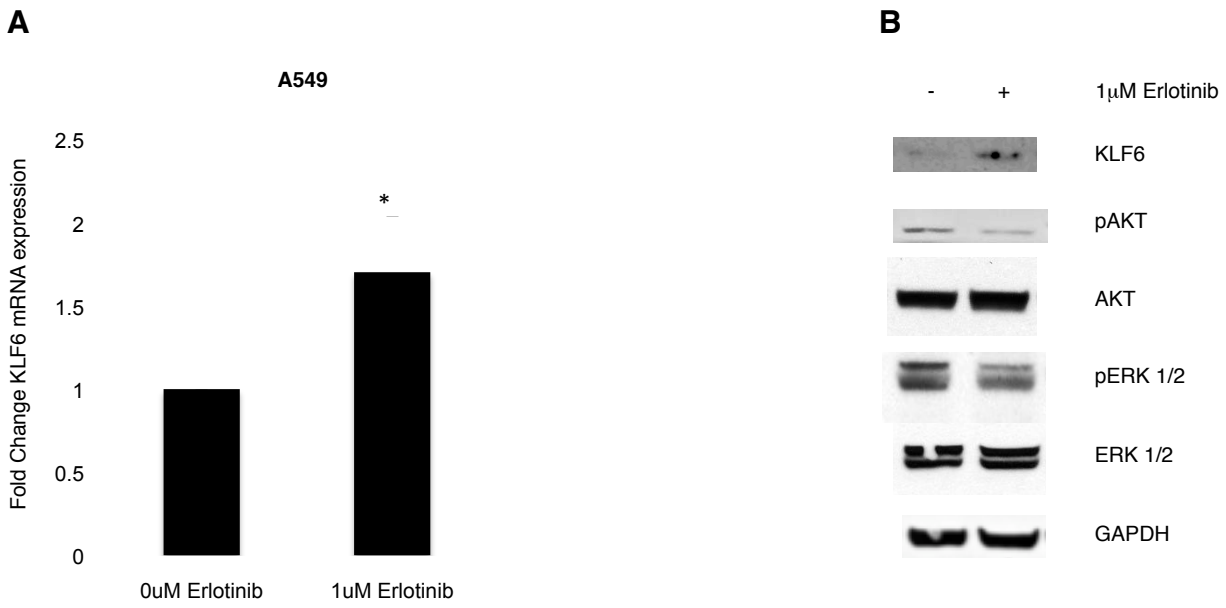

Supplemental Figure 4

Increase in KLF6 expression in A549 with 1μM treatment of erlotinib. **(A**) Quantitative real-time PCR for KLF6 mRNA expression levels in A549 cells after treatment with 1uM erlotinib **(B)** Western blot for KLF6, pAKT, AKT, pERK, and ERK in A549 cells after treatment with 1μM erlotinib

Mutation Status: EGFR/PI3K/PTEN K-Ras WT

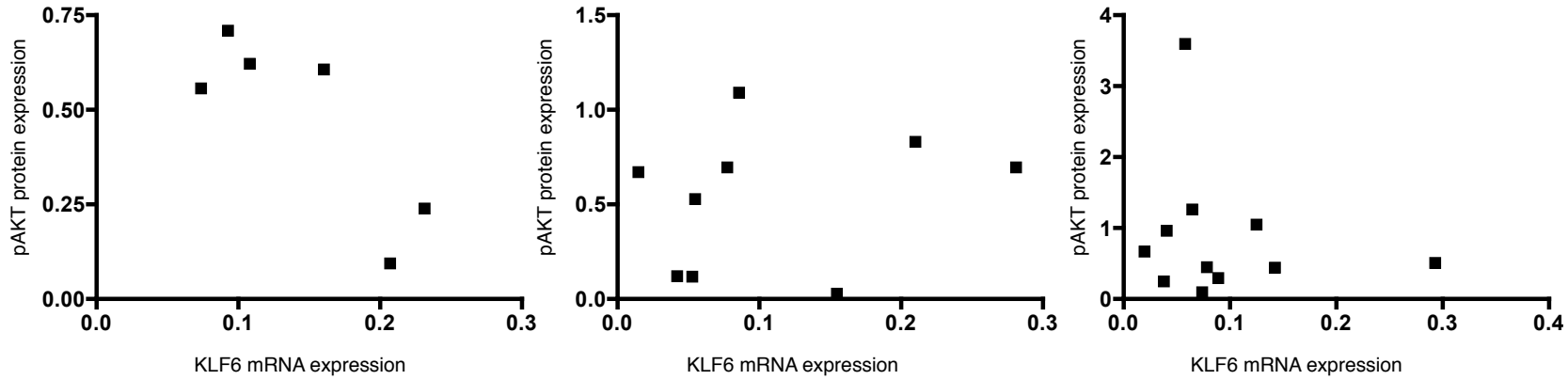

Parameter	KLF6
Number of XY Pairs	6
Pearson r	-0.8289
95% confidence interval	-0.9807 to -0.05257
P value (two-tailed)	0.0414
P value summary	*
Is the correlation significant? (alpha=0.05)	Yes
R squared	0.6870

Parameter	KLF6
Number of XY Pairs	9
Pearson r	0.2114
95% confidence interval	-0.5268 to 0.7678
P value (two-tailed)	0.5851
P value summary	ns
Is the correlation significant? (alpha=0.05)	No
R squared	0.04469

Parameter	KLF6
Number of XY Pairs	11
Pearson r	-0.1728
95% confidence interval	-0.7002 to 0.4766
P value (two-tailed)	0.6114
P value summary	ns
Is the correlation significant? (alpha=0.05)	No
R squared	0.02987

Supplemental Figure 5

Phospho-AKT expression is correlated with KLF6 expression in human primary lung adenocarcinomas**.** Patient-derived lung adenocarcinoma tumor samples with matched normal tissue adjacent to the retrieved tumor were evaluated for the presence of mutations in EGFR signaling pathway using a somatic mutation PCR-based array. Homogenized protein lysates from tumor samples were probed with a pAKT antibody and quantitation was performed via densitometry normalized against GAPDH expression. KLF6 mRNA expression was evaluated by qRT-PCR using validated wild-type KLF6-specific primers and normalized to three independent housekeeping genes (GAPDH, Actin, and 18S transcripts). pAKT and KLF6 levels showed a correlation (R^2=0.6870) in tumor samples with mutations present in EGFR, PI3K, or PTEN.

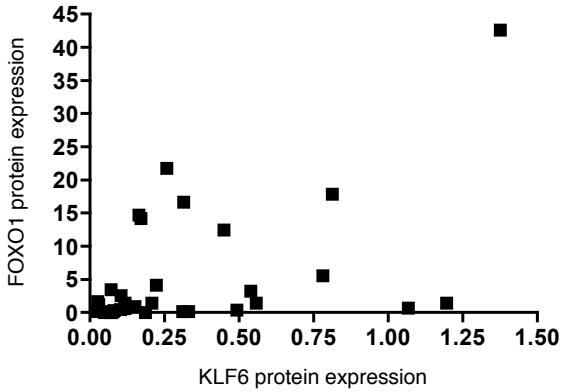

Parameter	Fold Change KLF6
Number of XY Pairs	33
Pearson r	0.4929
95% confidence interval	0.1800 to 0.7152
P value (two-tailed)	0.0036
P value summary	**
Is the correlation significant? (alpha=0.05)	Yes
R squared	0.2429

Supplemental Figure 6

FOXO1 expression is correlated with KLF6 expression in human primary lung adenocarcinomas. FOXO1 and KLF6 levels in a cohort of 13 patients were determined by western blotting and a positive correlation (R^2=0.4929) between FOXO1 and KLF6 expression was identified in this cohort of primary human lung adenocarcinoma tumor samples.

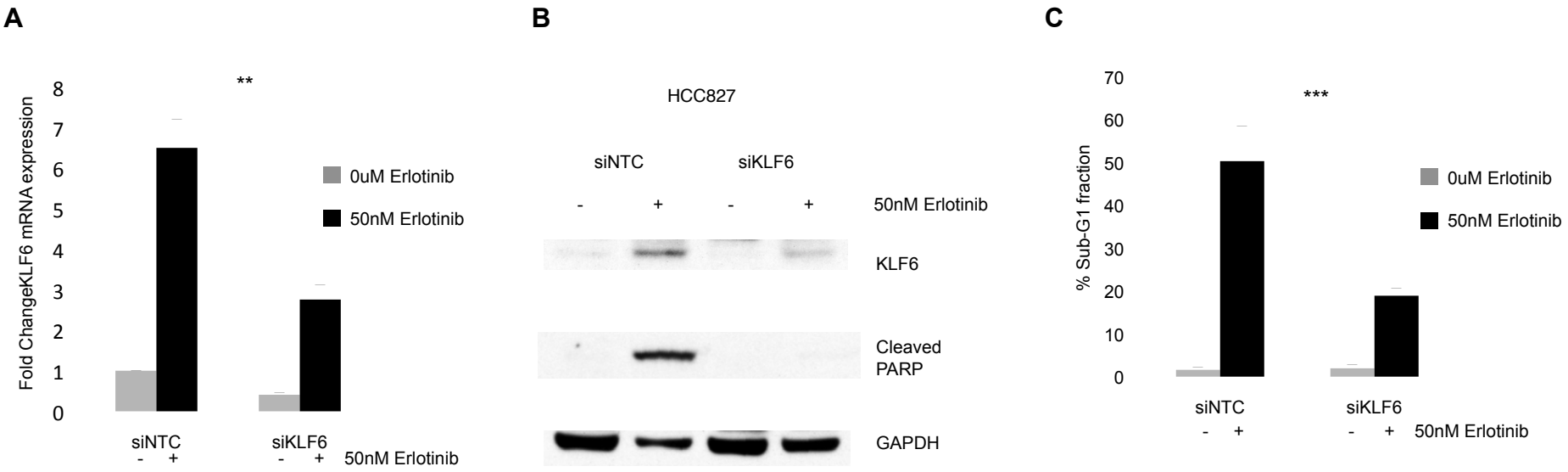

Supplemental Figure 7

Targeted reduction of KLF6 in the erlotinib-sensitive HCC827 cell line confers drug resistance in culture. **(A)** qRT-PCR for KLF6 mRNA expression normalized to GAPDH after transfection of HCC827 with 100mM sequence-specific KLF6 siRNA or scrambled siRNA control and subsequent treatment with 50nM erlotinib. **(B)** Western blot for KLF6 and cleaved PARP protein expression normalized to GAPDH after transfection of HCC827 with 100mM sequence-specific KLF6 siRNA or scrambled siRNA control and subsequent treatment with 50nM Erlotinib. **(C)** Cell cycle analysis using flow cytometry of the sub-G1 cell cycle fraction post propidium iodide staining after transfection of HCC827 with 100mM sequence-specific KLF6 siRNA or scrambled siRNA control and subsequent treatment with 50nM Erlotinib.

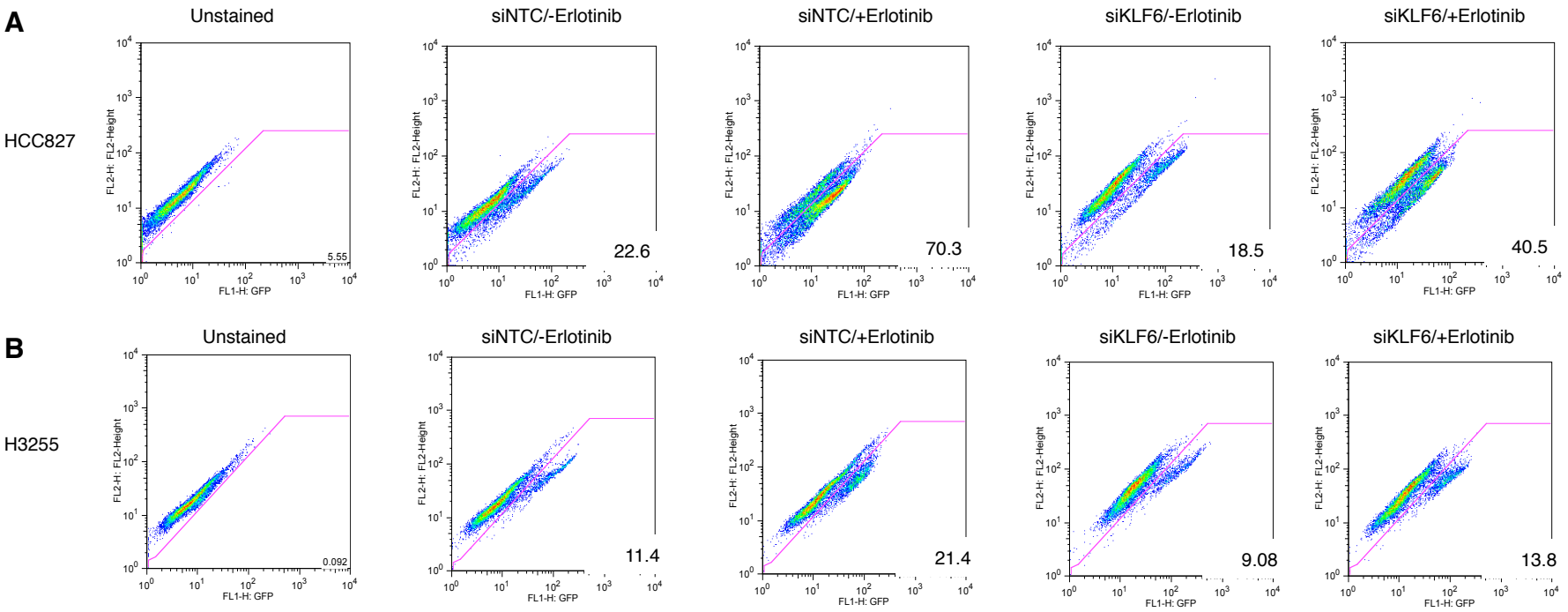

Supplemental Figure 8

Induction of apoptosis via Annexin V staining. Percent apoptosis (Annexin V positive staining) shown after transfection of **(A)** HCC827 and **(B)** H3255 cells with 100mM of sequence-specific KLF6 siRNA or scrambled siRNA control and subsequent treatment with 50nM erlotinib.

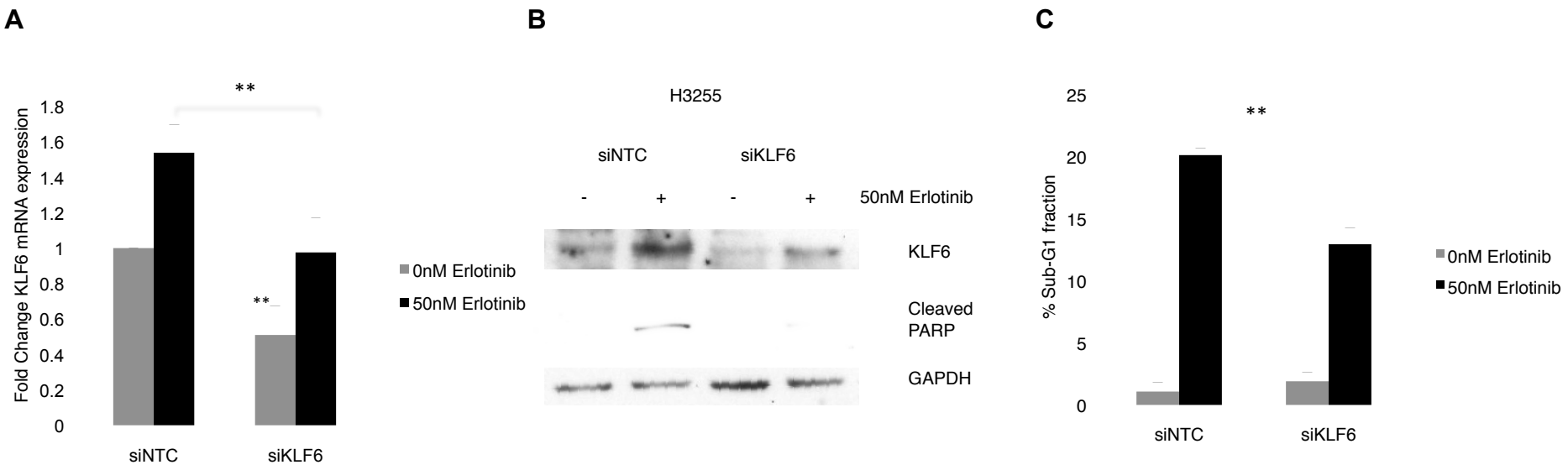

Supplemental Figure 9

Targeted reduction of KLF6 in the erlotinib-sensitive H3255 cell line confers drug resistance in culture. **(A)** qRT-PCR for KLF6 mRNA expression normalized to GAPDH after transfection of H3255 with 100mM sequence-specific KLF6 siRNA or scrambled siRNA control and subsequent treatment with 50nM erlotinib. **(B)** Western blot for KLF6 and cleaved PARP protein expression normalized to GAPDH after transfection of H3255 with 100mM sequence-specific KLF6 siRNA or scrambled siRNA control and subsequent treatment with 50nM Erlotinib. **(C)** Cell cycle analysis using flow cytometry of the sub-G1 cell cycle fraction post propidium iodide staining after transfection of H3255 with 100mM sequence-specific KLF6 siRNA or scrambled siRNA control and subsequent treatment with 50nM Erlotinib.

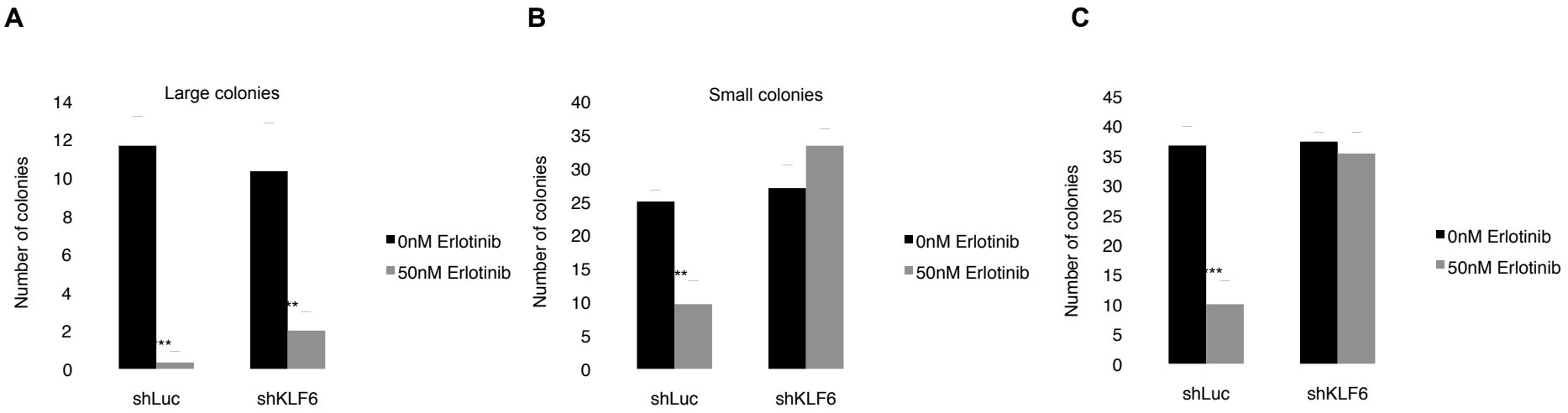

Supplemental Figure 10
Quantification of colony size and colony number in the HCC827 clonogenic assays. **(A**) Quantification of larger colonies. **(B**) Quantification of smaller colonies. **(C**) Quantification of total colonies are presented.

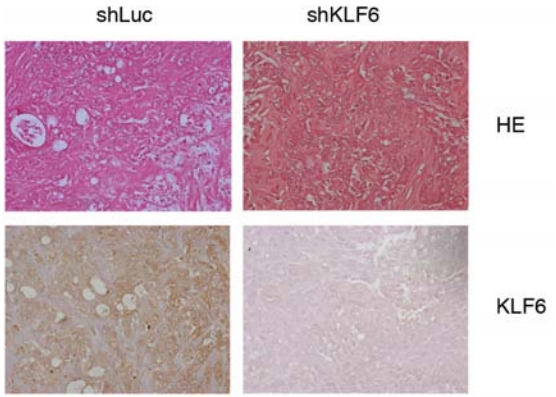

Supplemental Figure 11
Validation of KLF6 downregulation in xenograft model. Subcutaneous xenograft tumors, derived from $1x10^7$ shLuc-HCC827 or shKLF6-HCC827 lung adenocarcinoma cells injected into the right posterior flank of nude mice followed by an initial growth period of 14 days and subsequently treated with erlotinib. Paraffin histology sections stained for H&E and KLF6. Representative images shown (400x).

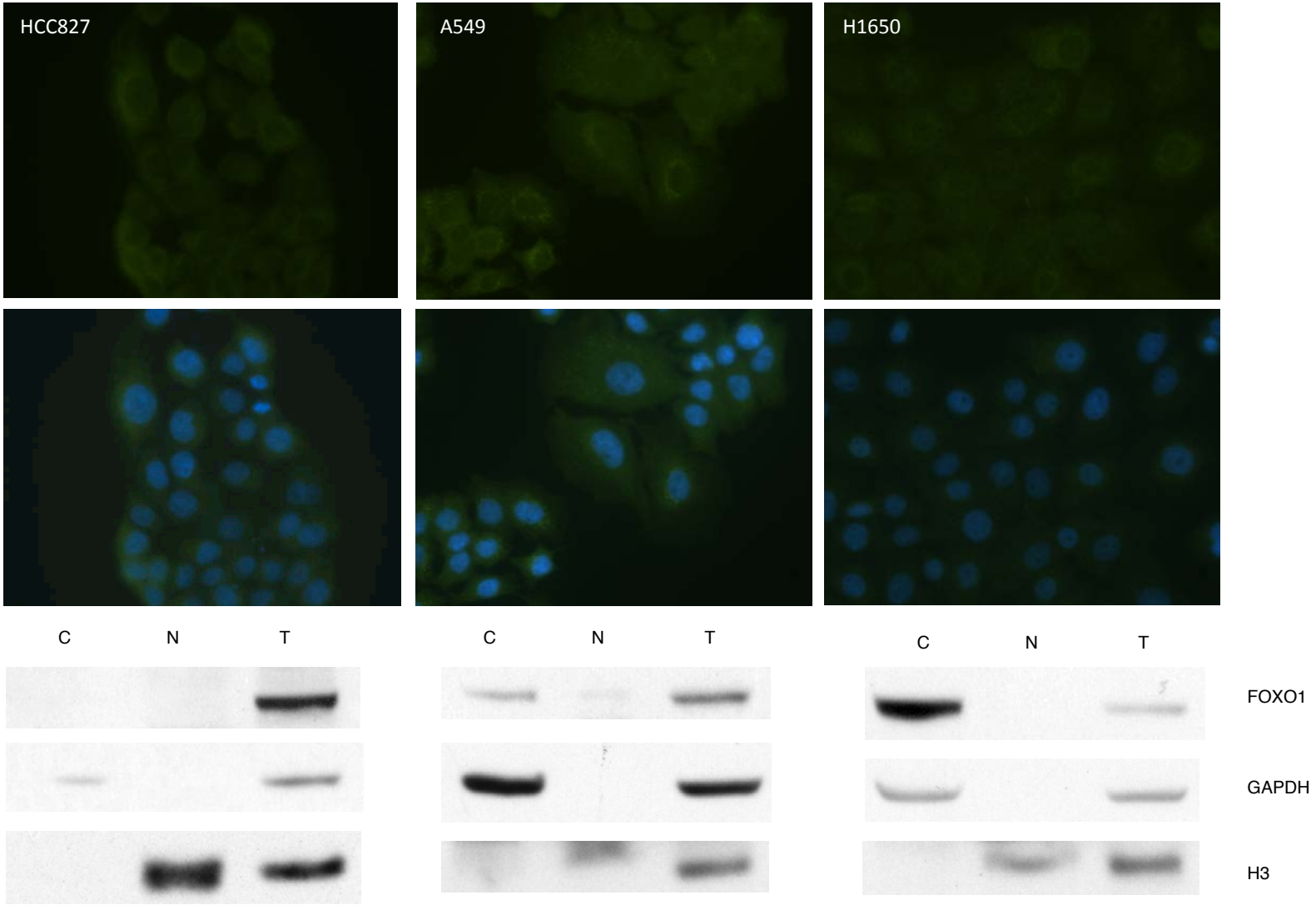

Supplemental Figure 12

FOXO1 localization in the HCC827, A549, and H1650 cell lines. Immunocytochemistry was performed to using FOXO1 antibody and DAPI counterstain to visualize the localization of FOXO1. Western blots for FOXO1, GAPDH, and KLF6. C: cytoplasmic; N: nuclear; T: total fraction.

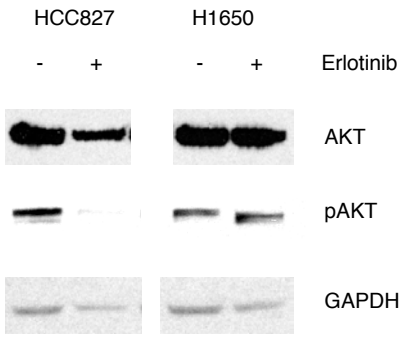

Supplemental Figure 13
The H1650 cell line is resistant to erlotinib via constitutive AKT activation. Western blot analysis for AKT, pAKT and GAPDH in cell lines HCC827 and H1650 after treatment with 50nM erlotinib for 24 hours.

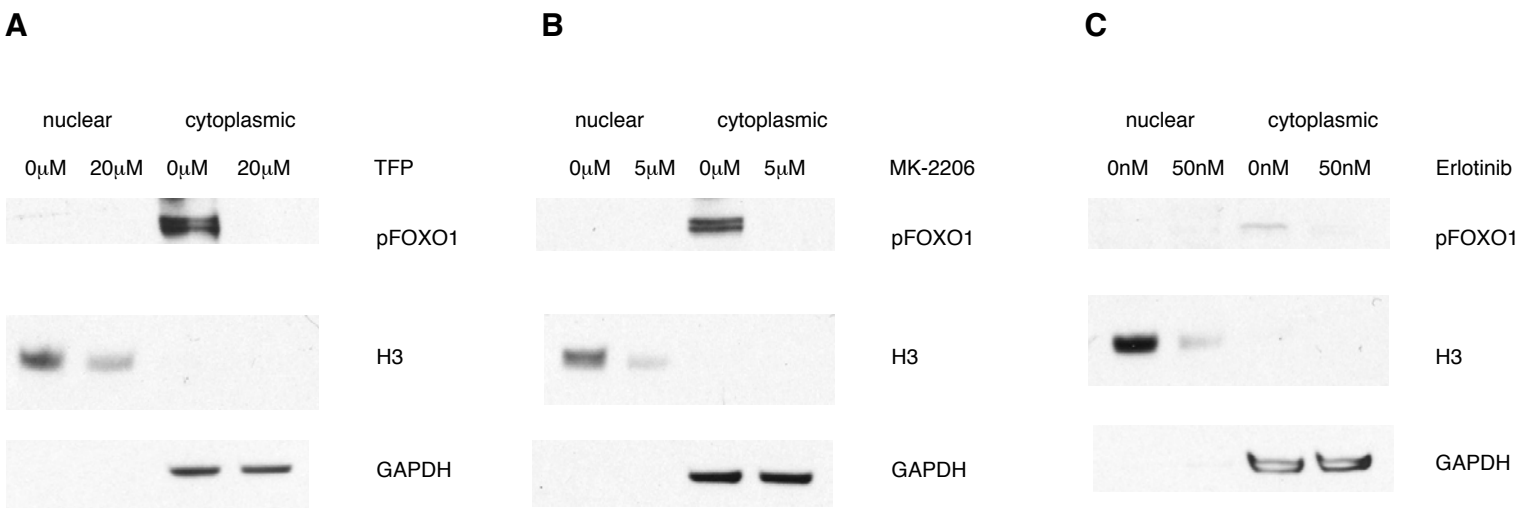

Supplemental Figure 14
Decrease in pFOXO1 upon treatment with TFP, MK-2206, or erlotinib. Western blot analysis for pFOXO1, H3, and GAPDH in cell lines H1650 cells treated with **(A)** TFP, **(B)** MK-2206 or **(C)** erlotinib and subjected to nuclear/ cytoplasmic fractionation.

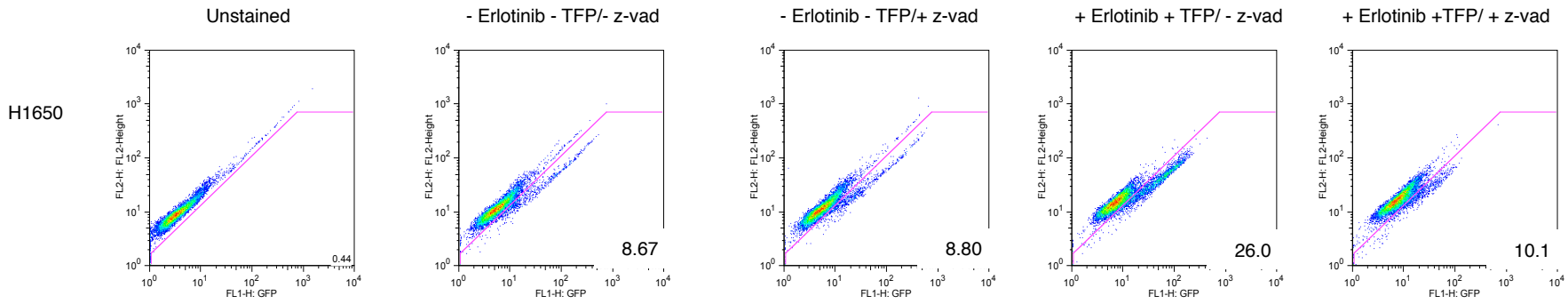

Supplemental Figure 15

Induction of apoptosis via Annexin V staining. Percent apoptosis (Annexin V positive staining) shown after treatment of H1650 cells with erlotinib in combination with TFP and subsequent addition of z-vad.

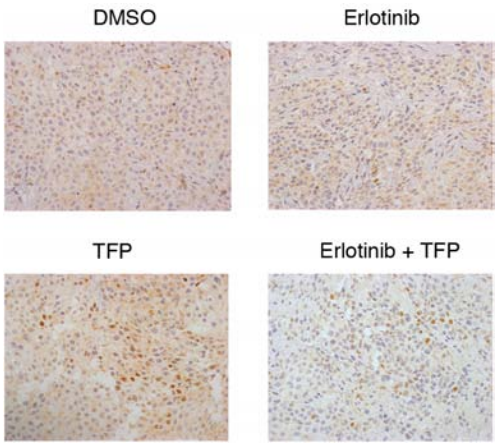

Supplemental Figure 16

Treatment with TFP alone or in combination with erlotinib results in nuclear localization of FOXO1. Xenograft tumors were derived from $5x10^6$ H1650 lung adenocarcinoma cells injected into the right posterior flank of nude mice. Following an initial growth period of 21 days, group tumor volume (n=14) averaged $200mm^3$ prior to beginning treatment. Mice were subsequently treated with DMSO (vehicle control), erlotinib (25 mg/kg), TFP (10mg/kg), and combination of TFP and erlotinib. Paraffin histology sections subjected to immunohistochemistry for FOXO1. Representative images are shown (40x).

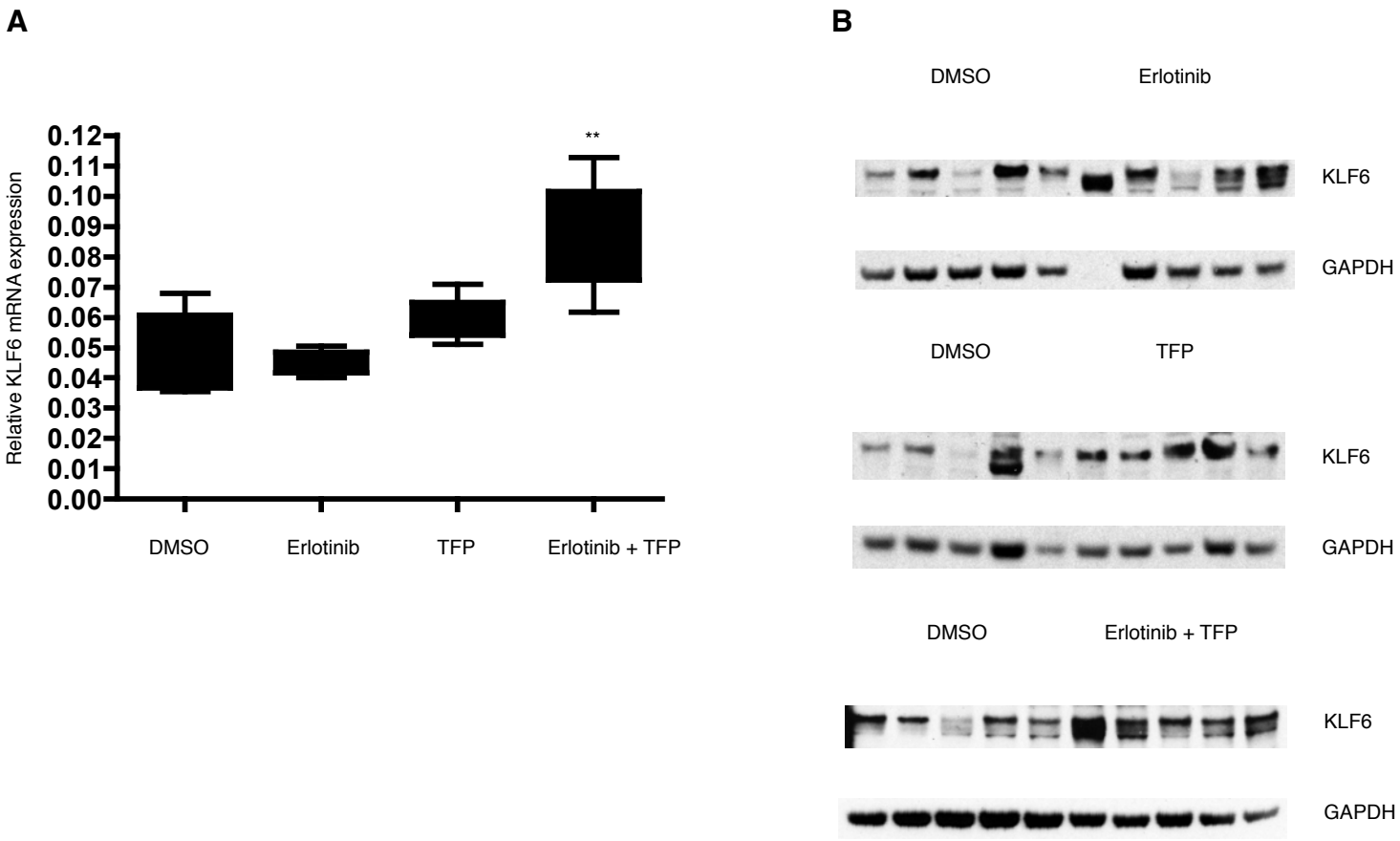

Supplemental Figure 17

Trifluoperazine and erlotinib administered in combination increases KLF6 expression. **(A)** qRT-PCR for KLF6 mRNA expression from tumors homogenized after the H1650-injected nude mice were sacrificed 24 hours after final treatment. **(B)** Western blot analysis of KLF6 expression in homogenized tumor samples. Lysate homogenates from treated and untreated tumors were run and probed in parallel (n=5), normalized to GAPDH.

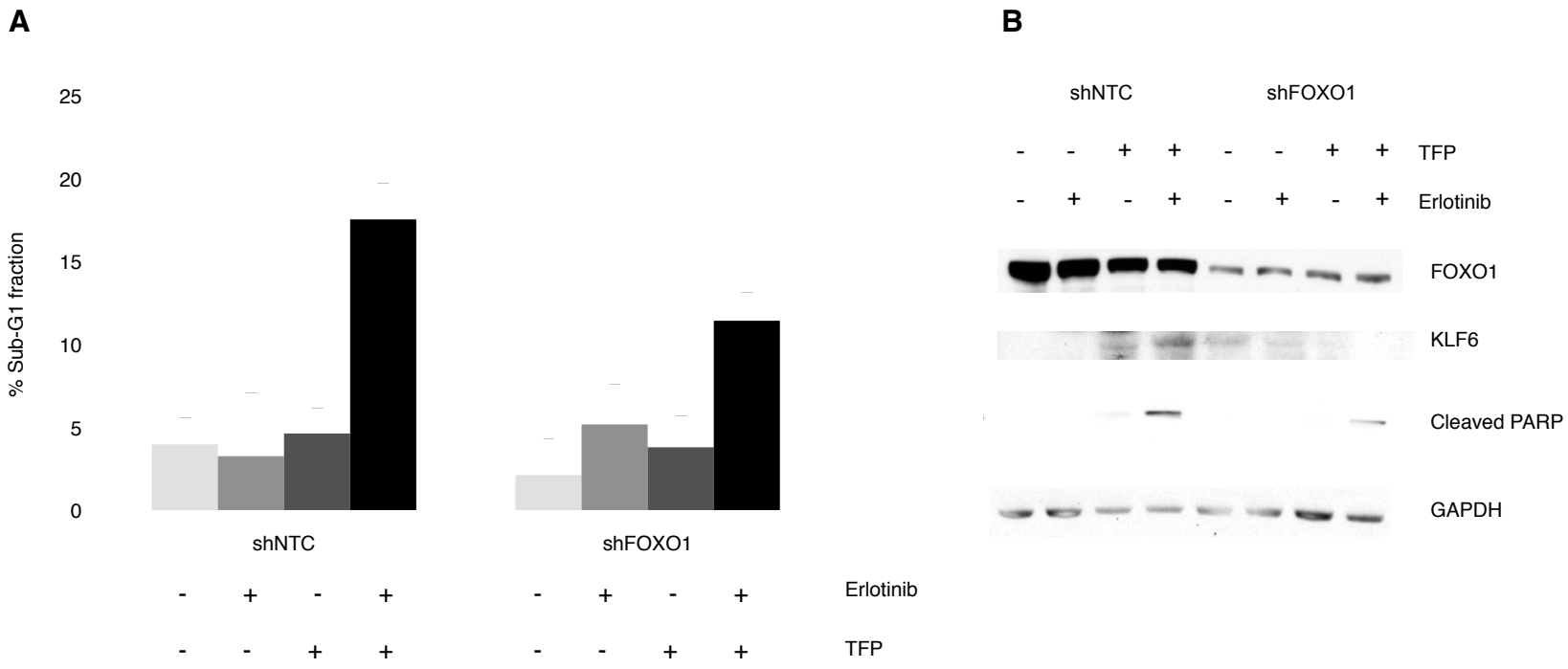

Supplemental Figure 18
Silencing of FOXO1 in the H1650 cell line confers drug resistance to TFP and erlotinib. **(A)** Cell cycle analysis using flow cytometry of the sub-G1 fraction post propidium iodide staining in the control cell line shNTC-H1650 and stable knockdown cell lines shFOXO1-H1650 after treatment with TFP and erlotinib. **(B)** Western blot for FOXO1, KLF6, and cleaved PARP in the control cell line shNTC-H1650 and stable knockdown cell lines shFOXO1-H1650 after treatment with TFP and erlotinib.

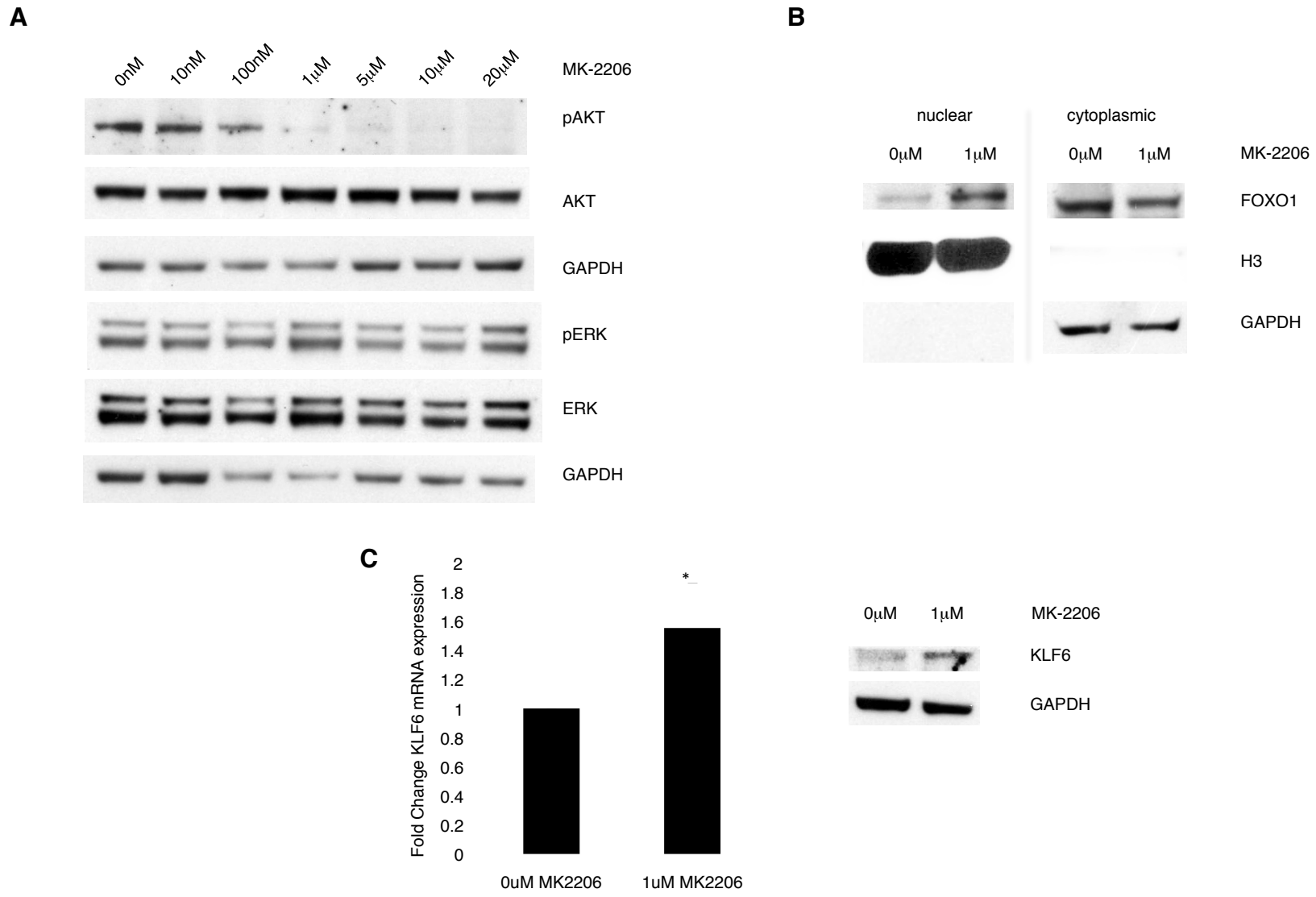

Supplemental Figure 19

Inhibition of FOXO1 nuclear export results in upregulation of KLF6 expression in A549. **(A)** Western blotting for pAKT, AKT, pERK, ERK in A549 cells after treatment with increasing doses of MK2206. **(B)** Western blot for FOXO1, H3 and GAPDH after nuclear cytoplasmic fractionation of the A549 cell line treated with 5μM MK2206. (H3: nuclear fraction control, GAPDH:cytoplasmic fraction control). **(C)** Quantitative real-time PCR and western blotting for KLF6 expression levels in A549 cells after treatment with MK-2206